Magnetic Nanowires for RF applications: Ferromagnetic Resonance and Permeability Characterization

Yali Zhang[1], Joseph Um[2], Wen Zhou[3], Bethanie Stadler[4], Rhonda Franklin[5]
University of Minnesota-Twin Cities, USA
[1]zhan4898@umn.edu, [2]umxxx023@umn.edu, [3]zhou0596@umn.edu, [4]stadler@umn.edu, [5]rfrank01@umn.edu

***Abstract*—Magnetic nanowires show promising potential in non-reciprocal device design and emerging areas like cells labeling in nano-medicine applications. One challenge, however, is how to obtain ferromagnetic resonance frequency (FMR) and complex permeability in a simplistic manner. In this study, a through line and short-circuited CPW circuits were used to obtain FMR in DC magnetic field and frequency domains, respectively. Factors were investigated to understand how magnetic field absorption is affected by sample placement on the circuit, how FMR is impacted by the angle between wire axis and DC field, and how complex permeability can be extracted from the reflection data. Using the "four steps" method which was commonly used for thin films [1-3], we obtain FMR of 27 GHz at 0.4T and complex permeability values of μ' =7 and μ'' =4.5, respectively for cobalt nanowires (pH=2).**

***Keywords* — Magnetic nanowires, coplanar waveguide, ferromagnetic resonance, vector network analyzer.**

I. Introduction

Magnetic nanowire properties are unique due to its high shape anisotropy along the wire axis. Its properties can also be engineered. The magnetic properties of nickel and cobalt (Co) nanowires were initially studied [4], [5] for its DC and AC properties in the 0-40GHz. The conventional use of magnetic nanowire materials was based on DC properties in applications such as magnetic random access memory device (MRAM) [6], hard disk drive (HDD) [7] and cell manipulation technology [8]. More recently, the AC properties have shown promise and have been used in non-reciprocal devices [9] and in nano-biolabeling systems design [10]. However, procedures are limited about how to characterize magnetic nanowire material AC properties like ferromagnetic resonance (FMR) and permeability at RF and microwave frequencies in a straightforward way.

FMR stems from the natural precession of magnetization in a magnetic material exposed to specific combinations of DC magnetic field and orthogonal AC magnetic field. Thus, it is a powerful technique for detecting and distinguishing magnetic materials.

Waveguide cavity [11], microstrip [12] and coplanar waveguide (CPW) [5] are typical microwave circuit structures that can provide an AC magnetic field which interacts with magnetic nanowires. CPW has broader measurement frequency range and offers ease of use with measurement samples compared with waveguide cavity. CPW also provides a stronger AC magnetic field on top of the circuit board, which is desired for sample characterization, compared with microstrip.

FMR measurement approaches include lock-in detection method, pulse perturbation method, and VNA-FMR method [13]. Herein, the VNA-FMR method was adopted with both short-circuited and through-line CPW measurement boards. Measurements were conducted with both frequency sweep and static magnetic field sweep. In this paper, the role of chip placement and angle dependence between wire axis and DC field will be discussed as it relates to FMR. Then, the method used to extract magnetic nanowire array permeability will be described and used to determine the FMR and complex permeability of Co nanowires.

II. Magnetic Nanowire Sample Description and Experimental Set up for FMR Detection

An aluminum oxide (AAO) template was used to grow cobalt (Co) nanowires with 12% porosity and 40nm diameter pores. A 7nm Ti adhesion layer and a 300 nm thick Cu electrode were sputtered on one side of AAO. The pH value of precursor solution is 2 which makes the nanowires have no crystalline anisotropy. See [10] for the electrodeposition fabrication process. The cross-sections of Co nanowire samples are shown in Fig. 1a and Fig. 1b.

Two nanowire samples were used: (a) Co72 and (b) Co80. Nanowire lengths for Co72 and Co80 are 15.5μm and 28.2μm, respectively.

The chips dimensions (l=length and w=width) for Co72-A (l=2.8 and w=2), Co72-B (l=1.958 and w=0.331) and Co80 chip (l=3.698 and w=0.423) are in millimeters.

For Co72, the hysteresis loop measurements indicate the saturation magnetization (M_s) is 1440emu/cc and anisotropy field (H_a) is 4446 Oe for permeability extraction.

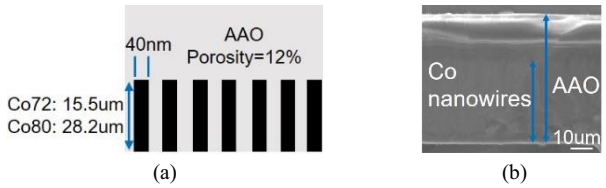

(a) (b)

Fig. 1. (a) Cross section of Co nanowire sample – wires (black), (b) SEM photo of cross-section of Co nanowire sample.

The z-shaped and short-circuited CPW test circuits shown in Fig. 2a and Fig. 2b were designed on 10 mil Duroid 5880LZ ($\varepsilon_r = 2$) with signal line width of 16.5mil and gap width of 5mil. The trace length is 7.8mm for the short-circuited board and 6.8cm for the z-shaped board.

(a) (b)

Fig. 2. (a) short-circuited CPW board, (b) z-shaped through-line CPW board.

In all experiments, a sample was put above the CPW board and attached using vacuum grease for easy removal. Then the sample was placed between two poles of an electromagnet that supplied a DC field. An Anritsu 37369D VNA provided AC signal to induce the AC magnetic field and to detect the FMR absorption in the transmission (S_{21}) and reflection (S_{11}) coefficient of the circuits.

Here, two domains were used for detecting FMR frequency: (a) DC field and (b) frequency. For detecting the FMR in the DC field domain, the supplied AC frequency was fixed and located in the range of 5 GHz to 40 GHz and the DC field was swept from +1.5T to -1.5T at a rate of 250 Oe/s. For detecting the FMR in the frequency domain, the DC field was fixed in the range of 0.0T to 1.5T and the frequency was swept from 17GHz to 40 GHz.

To reduce the interference from other magnetic materials in the testing system, nonmagnetic cables (Cinch Connectivity Solutions) were used for testing. The flexible nonmagnetic cables, however, were sensitive to bending compared to the semi-rigid measurement cables during calibration. Thus, two-port measurements were referenced to the VNA ports (i.e. without calibrating out the cable); whereas one-port measurements were calibrated since the single cable could be fixed to a 3D printed fixture without significant movement during calibration.

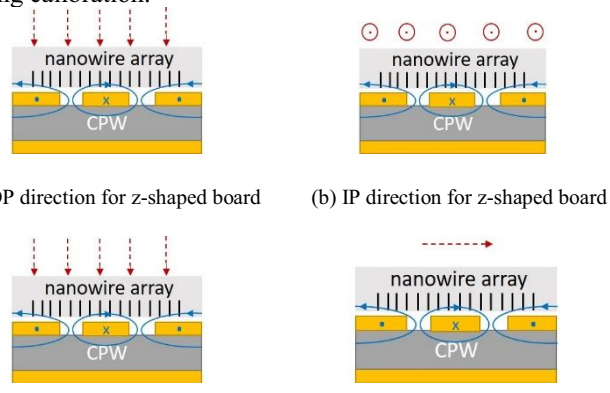

(a) OP direction for z-shaped board (b) IP direction for z-shaped board

(c) OP direction for short-circuited board (d) IP direction for short-circuited board

Fig. 3. A schematic of the cross sections of CPW boards to show field distribution in OP and IP direction. The red dashed line and red circle represent the DC field direction, the blue solid line represents the AC field direction and the black line is nanowire axis. All cross sections are from the middle of the z-shaped board and short-circuited board.

Typical FMR detection measurements are obtained for DC magnetic field direction in the out-of-plane (OP) direction and in-plane (IP) direction. The DC field and AC field distribution are shown in Fig. 3.

III. Measurement and Results Analysis

A. FMR results in DC field domain

Firstly, the FMR of Co72-A was measured on z-shaped board at different DC field to wire axis angles of 0° (OP), 30°, 60° and 90° (IP) to show angle dependence of FMR results.

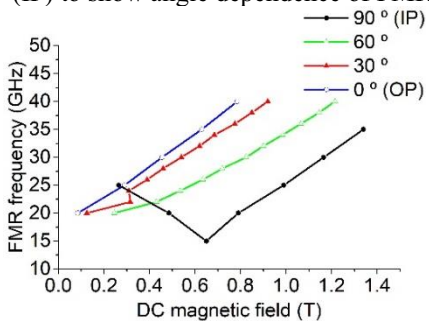

Fig. 4. The FMR frequency versus DC field pattern at 0° (OP), 30°, 60° and 90° (IP).

Fig. 4 shows data of FMR versus DC field for angles between wire axis and DC field. At 0° (OP), the FMR frequency increases linearly with DC field strength; whereas at 90° (IP), FMR frequency shows minimum value around 0.65 T. A gradual transition can be observed at 30° and 60°. Magnetization prefers to align with the wire axis due to the strong shape anisotropy presented in the nanowire array. When the angles of the DC field to the wire axis increase, it becomes harder to achieve saturation which requires higher DC field.

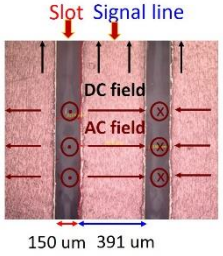

Fig. 5. The top view of CPW board

Secondly, the sample placement on the CPW line is also important. The Co80 sample was measured on z-shaped board at IP direction (90°) to show the optimal angle between AC field and magnetization for detecting the FMR frequency.

In Fig. 6a, the low DC field and high DC field regions are separated by a transition point, the red dashed line intersects with a black line at two FMR frequencies that are pointed out in Fig. 6b.

In Fig. 6b, there are two FMR absorptions in IP orientation regardless of sample placement on the slot or signal line. One absorption occurs in the low DC field region where the nanowire magnetization is dominated by shape

anisotropy effect and the other occurs in the high field region where the magnetization is aligned with DC field in IP orientation (Fig. 6a).

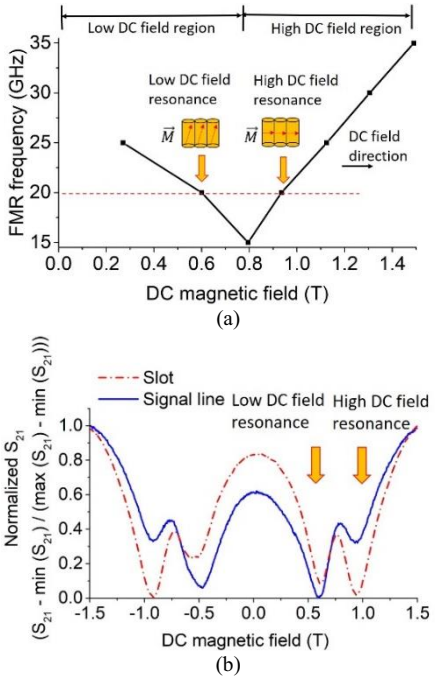

Fig. 6. (a) FMR frequency versus DC field in IP direction, (b) The comparison between the sample on the slot and signal line at 20GHz in IP direction.

When the sample is on the signal line, the AC field is orthogonal to the magnetization in both low and high DC field regions. When the sample is on the slot, however, the AC field is orthogonal to magnetization in the high DC field region but close to parallel in the low field region. Unfortunately, the non-orthogonality between AC field and magnetization in the low field region leads to the weaker absorption which flips the strength relationship between the low field resonance and high field resonance. Thus, for efficient absorption of FMR, AC field should be perpendicular to the magnetization.

Finally, Co72-B was measured in Fig. 7 on the z-shaped and short-circuited board in the DC field domain to validate that the FMR frequency of the sample on the two boards are similar. Thus, the short-circuited board will be used for easier extracting various material properties and de-embedding the cable and connector effects.

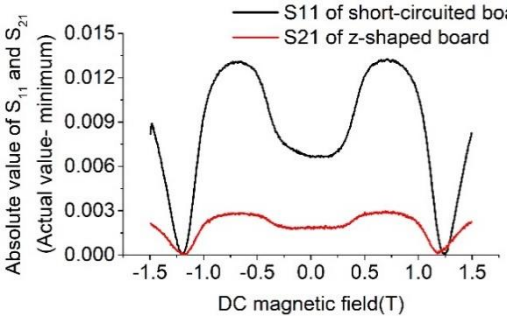

Fig. 7. The FMR measurement of the Co72 on z-shaped board and short-circuit board at 26GHz in IP orientation.

B. *Permeability extraction from FMR results in frequency domain*

In frequency domain, identifying the FMR absorption peak is a challenge due to RF background noise. Fig. 8 shows S_{11} of short-circuited CPW with AAO sample and Co72-B sample at 0.4T and 0.5T. The additional reduction in S_{11} with the Co72-B sample compared to the empty AAO suggest that FMR is present. However, it is not adequate to determine the specific FMR frequency due to additional board resonances. Thus, the known "four steps" method [1-3] was applied here to determine the FMR frequency and extract the permeability of Co72-B.

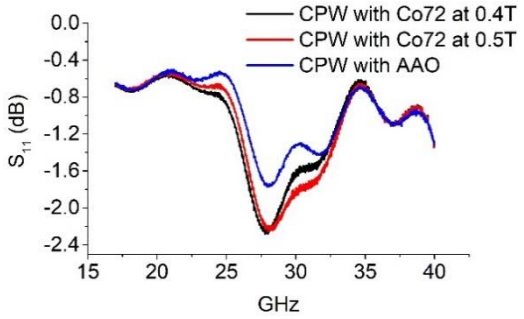

Fig. 8. The S_{11} measurement of the CPW board with nanowire sample at 0.4T, 0.5T and CPW board with same size AAO in OP direction.

Using the "four steps" method, first, a calibration was performed to remove cables and connector effects. A one port VNA calibration was performed to shift the reference plane to the input of the test circuit connector. Then, the S_{11} value of two short-circuited CPW test boards (i.e. lengths of 7.8mm and 5.8mm) was measured to remove the connector effects. Second, the empty test board was measured to obtain the effective permittivity of short-circuited CPW test board. Third, the CPW test board was measured with AAO template to obtain effective permittivity of board with AAO. And finally, the test board with nanowire array sample was measured to obtain the effective permeability of the test board with nanowire sample. The last measurements were used to extract the relative permeability of the nanowires based on the effective permittivity and effective permeability value from the previous steps. This equation [2]

$$\mu'_{initial} = \frac{Ms}{Ha} + 1 \qquad (1)$$

was used for calibrating the initial real part of relative permeability in low frequency range using M_s of 1440 emu/cc and H_a of 4446Oe.

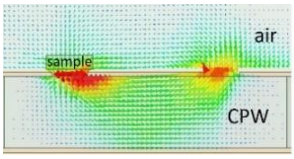

Fig. 9. HFSS simulation for AC magnetic field distribution of CPW board at cross section. Red and green arrows represent the AC magnetic field strength of 270A/m and 109A/m respectively.

In third and fourth steps, the AAO and magnetic nanowires sample were put above the left slot of the CPW board in OP direction of DC field to reach the maximum AC field region as seen in Fig .9. It is observed that the sample is slightly wider than the gap and it is believed that the sample edges above the signal line absorb the AC field energy due to the orthogonal relationship between magnetization and AC field on the signal line.

The relative permeability, $\mu = \mu' - j\mu''$, of Co72-B at 0.4T in OP orientation is shown in Fig. 10. The FMR frequency for Co72-B is 27GHz based on the peak of μ'', which is not obvious from S_{11} Fig. 8. Fig. 10 shows that the real part of relative permeability is 7 and the imaginary part is 4.5 at FMR frequency.

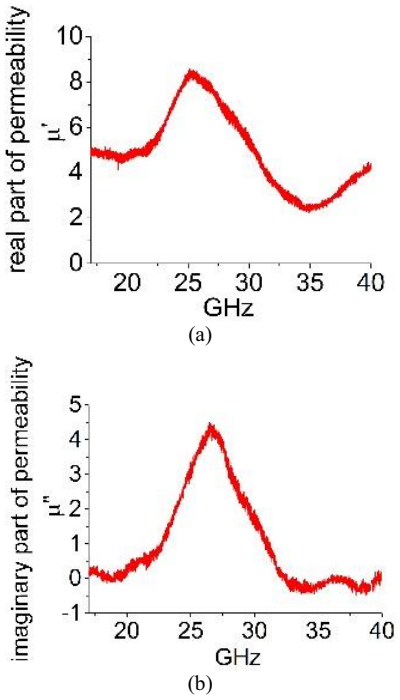

Fig. 10. (a) The real part of permeability μ' for nanowire array at 0.4T in OP direction, (b) The imaginary part $\mu''$of permeability for nanowire array at 0.4T in OP direction. The FMR frequency for Co72-B at 0.4 T is 27GHz.

IV. Conclusion

This paper presents two measurement techniques for characterizing magnetic nanowires. In DC field domain measurement, the angle dependence study shows the capability to predict the FMR frequency range for randomly oriented nanowires. The placement comparison experiments show the best angle relationship between magnetization and AC field should be orthogonal. In frequency domain measurement, the FMR frequency and permeability of nanowire sample were obtained by applying the "four steps" method commonly used for magnetic thin films. These studies provide a complete process for obtaining magnetic nanowires properties that are needed for a broad range of RF applications, such as nanolabels for nanomedicine and non-reciprocal devices for communications.

Acknowledgment

This work was supported by the National Science Foundation Award ECCS #1509543, MN Futures of the University of Minnesota, the Skippy Frank Fund for Life Sciences and Translational Research, and Animal Cancer Care and Research Program of the University of Minnesota.

Portions of this work were conducted in the Minnesota Nano Center, which is supported by the National Science Foundation through the National Nano Coordinated Infrastructure Network, Award Number NNCI -1542202.

References

[1] V. Bekker, K. Seemann, H. Leiste, "A new strip line broad-band measurement evaluation for determining the complex permeability of thin ferromagnetic films", *Journal of Magnetism and Magnetic Materials*, Vol. 270, 2004.

[2] Y. Liu, L. Chen, C. Y. Tan, H. J. Liu and C. K. Ong, "Broadband Complex Permeability Characterization of Magnetic Thin Films using Shorted Microstrip Transmission-Line Perturbation", *Review of Scientific Instruments*, Vol. 76,2005.

[3] J. Wei, H. Feng, Z. Zhu, Q. Liu and J. Wang, "A short-circuited coplanar waveguide to measure the permeability of magnetic thin films: Comparison with short-circuited microstrip line", *Review of Scientific Instruments*, Vol. 86, 2015.

[4] A. Fert, L Piraux,, "Magnetic nanowires", *Journal of Magnetism and Magnetic Materials,* Vol. 200, Issues 1–3, 1999.

[5] M. Sharma, S. Pathak and M. Sharma, "FMR Measurements of Magnetic Nanostructures", *Ferromagnetic Resonance*, 2013.

[6] C. T. Boone, J. A. Katine, M. Carey, J. R. Childress, X. Cheng and I. N. Krivorotov, "Rapid domain wall motion in permalloy nanowires excited by a spin-polarized current applied perpendicular to the nanowire", *Physical Review Letters* 104 (2010) 097203.

[7] S. Parkin, M. Hayashi, L. Thomas, "Magnetic Domain-Wall Racetrack Memory", *Science*, Vol. 320, 2008.

[8] A. Hultgren, M. Tanase, C. S. Chen, G. J. Meyer, D. H. Reichm, "Cell manipulation using magnetic nanowires", *Journal of Applied Physics*, Vol.93, 2003.

[9] M. Darques, J. Spiegel, J. De la Torre Medina, I. Huynen, L. Piraux, "Ferromagnetic nanowire-loaded membranes for microwave electronics", *Journal of Magnetism and Magnetic Materials*,Vol. 321, 2009.

[10] W. Zhou, J. Um, Y. Zhang, A. Nelson, B. Stadler and R. Franklin, "Ferromagnetic Resonance Characterization of Magnetic Nanowires for Biolabel Applications," *2018 IEEE International Microwave Biomedical Conference (IMBioC)*, Philadelphia, PA, 2018.

[11] A. Sklyuyev, M. Ciureanu, C. Akyel, P. Ciureanu, D. Menard and A. Yelon, "Measurement of Complex Permeability of Ferromagnetic Nanowires using Cavity Perturbation Techniques," *2006 Canadian Conference on Electrical and Computer Engineering*, Ottawa, Ont., 2006, pp. 1486-1489

[12] A. Encinas-Oropesa, M. Demand, L. Piraux, I. Huynen, and U. Ebels, "Dipolar interactions in arrays of nickel nanowires studied by ferromagnetic resonance," *Physical Review Letters*, Vol. 63, no. 10, 2001.

[13] S.S Kalarickal, P. Krivosik, M. Wu, C.E. Patton, M.L. Schneider, P. Kabos, T.J. Silva, J.P. Nibarger, "Ferromagnetic resonance linewidth in metallic thin films: Comparison of measurement methods", *Journal of Applied Physics,* 2006